The Nanomechanical Properties of Polystyrene Thin Films Embedded with Surface-grafted Multiwalled Carbon Nanotubes

Chih-Chun Hsiao, Tian Shyng Lin, Ling Yu Cheng, Chen-Chi M. Ma,† and Arnold C.-M. Yang*

Department of Materials Science and Engineering and Department of Chemical Engineering, National Tsing Hua University, Hsinchu 30043, Taiwan

Received July 31, 2004; Revised Manuscript Received March 6, 2005

ABSTRACT: Thin polystyrene (PS) films embedded with multiwalled carbon nanotubes (MWNTs) grafted with PS chains were prepared via solution casting, and the nanomechanical behavior of the thin films was probed by using AFM, TEM, and SEM. Percolated network of entangled nanotubes was observed to be well-dispersed in the PS thin films, and the films demonstrated strikingly different mechanical properties as compared to the pristine PS film. The MWNT/PS films were very tough showing no microfracture at large strains beyond 20%. Although crazes of similar microstructure to those in pristine PS were developed upon stretching, they were short and narrow with a width no more than approximately 2 μm. AFM analyses revealed that crazes grew by following a micronecking mechanism, similar to that commonly observed in neat polymers, but craze widening was substantially restricted. As a result, nucleation of new crazes became the dominant process over widening of the existing crazes as the applied strain increased. No nanotubes were observed inside crazes; they appeared to be excluded from craze fibrillation and were observed to accumulate at the craze boundaries. The growth of crazes in the MWNT/PS films was constrained by the nanotubes too rigid to be drawn into the crazes during the deformation.

Introduction

The chain behavior of macromolecules in the glassy state dictates the physical properties in a wide spectrum of polymer applications. A glassy polymer chain first deformed uniformly and elastically upon stretching until it yielded, commencing the plastic deformation afterward.[1] Yielding, when appeared in the forms of crazes or shear deformation zones, was found to follow the micronecking mechanics.[3] Crazes, commonly observed in the deformed brittle polymers, are cracklike defects that are load bearing[3−12] and possess a fibrillar microstructure. Here, we attempted to use carbon nanotubes finely dispersed into the polymer chain network to investigate the interactions between the glassy chains and the entanglement network of the nanotubes. The results can provide valuable insights toward the chain behavior of glassy polymers.

Carbon nanotubes have widely been touted as a superior candidate for uses as fillers in composite materials because of their extremely high Young's modulus, stiffness, flexibility, conductivity, and field emission properties.[13] Much research had used nanotubes as fillers in thermoplastics or epoxy matrixes which demonstrated greatly enhanced mechanical,[14,15] electrical,[16,17] and thermal[18,19] properties. It also had been shown that with only 1 wt % multiwalled carbon nanotubes (MWNTs) added as the filler, huge increases, 36−42%, in the elastic modulus of the composites could be resulted.[20] Small-diameter MWNTs were reported as the best candidates for polymer reinforcement.[21] However, the dispersion of the fine nanoscale nanotubes in polymers has been proved to be a formidable challenge. The composites would demonstrate inferior performances if the nanotubes were poorly dispersed. Furthermore, the adhesion between the nanotubes and the polymer matrix also plays a vital role in the reinforcement mechanisms. In a separate paper, we described how the MWNTs can be successfully dispersed into a polystyrene matrix by surface grafting the nanotubes with polystyrene chains.[22] In this paper, we report how the dispersed nanotubes influence the nanomechanical properties of the glassy polymers.

For this study, polystyrene was used as the polymeric matrix in the nanocomposites reinforced with the PS-grafted MWNTs. It was expected that adding a stiff PS-grafted MWNT would dramatically alter the stress transfer network of polymer chains. The performance of the mechanical properties of the composite films that resulted from the interactions between the MWNT network and polymer entanglement networks were reported. In addition, the nanomechanical properties of the MWNT/PS composite film were probed by using AFM analysis.[11]

Experimental Procedures

Monodisperse polystyrene ($M_w/M_n = 1.3$) of molecular weight $M_w = 2\,000\,000$ (Pressure Chemical Co., U.S.A.) was used as the polymeric matrix for this study. The MWNTs (DESUN Nano Co., Taiwan) used in this study were found to have an average outer diameter around 30 nm (Figure 1a) and a length of 10−30 μm. Aggregates were commonly observed in the as-received MWNTs samples (Figure 1b). The method of grafting PS chains onto the side walls of MWNTs were reported in a separate paper.[22] The PS-grafted MWNTs were mixed, by approximately 1.5 wt % in weight, with the PS in toluene solution. The MWNT/PS films were spun cast from the solution, and the film thickness was controlled to be around 0.35 μm. The MWNT/PS films were floated off the substrate on distilled water and bonded onto supporting copper grids. After following the proper bonding procedure,[23] the specimen was mounted in a strain jig and stretched under an optical microscope to observe the growth of local deformation zones (crazes or shear deformation zones, SDZ). The stretched MWNT/PS films were then examined under an AFM (Digital

* Author to whom correspondence should be addressed. E-mail: acyang@mse.nthu.edu.tw.
† Department of Chemical Engineering.

10.1021/ma048413y CCC: $30.25
Published on Web 04/21/2005

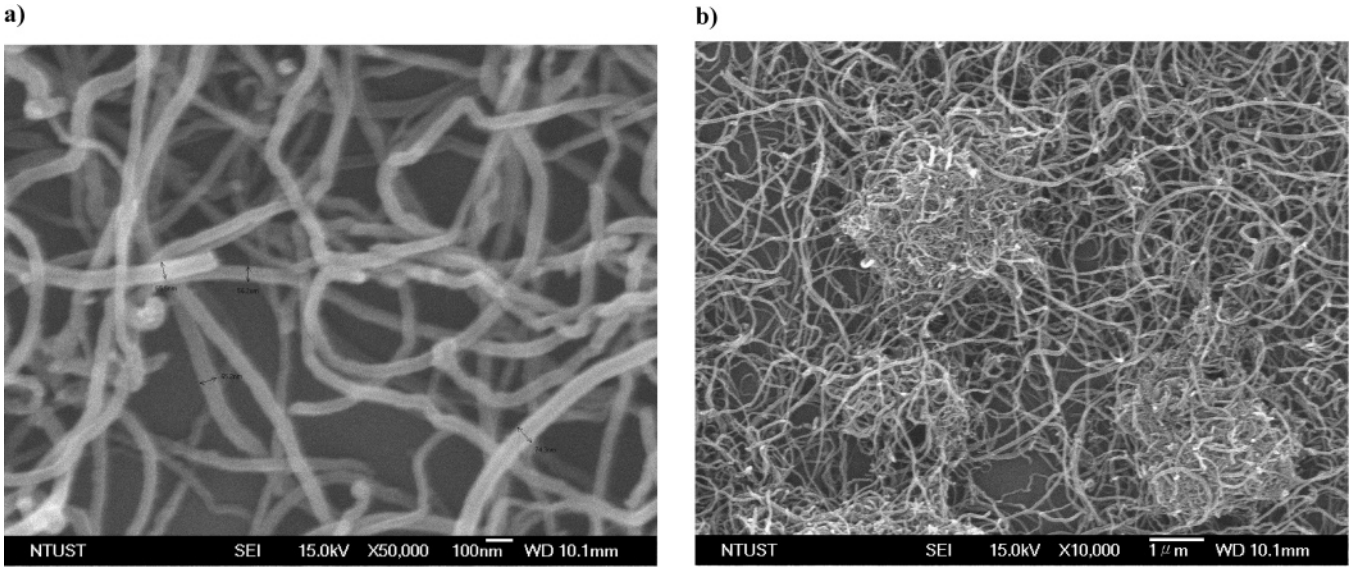

Figure 1. SEM micrographs of the MWNTs as received showing: (a) the entangled tube mass, and (b) aggregates of MWNTs.

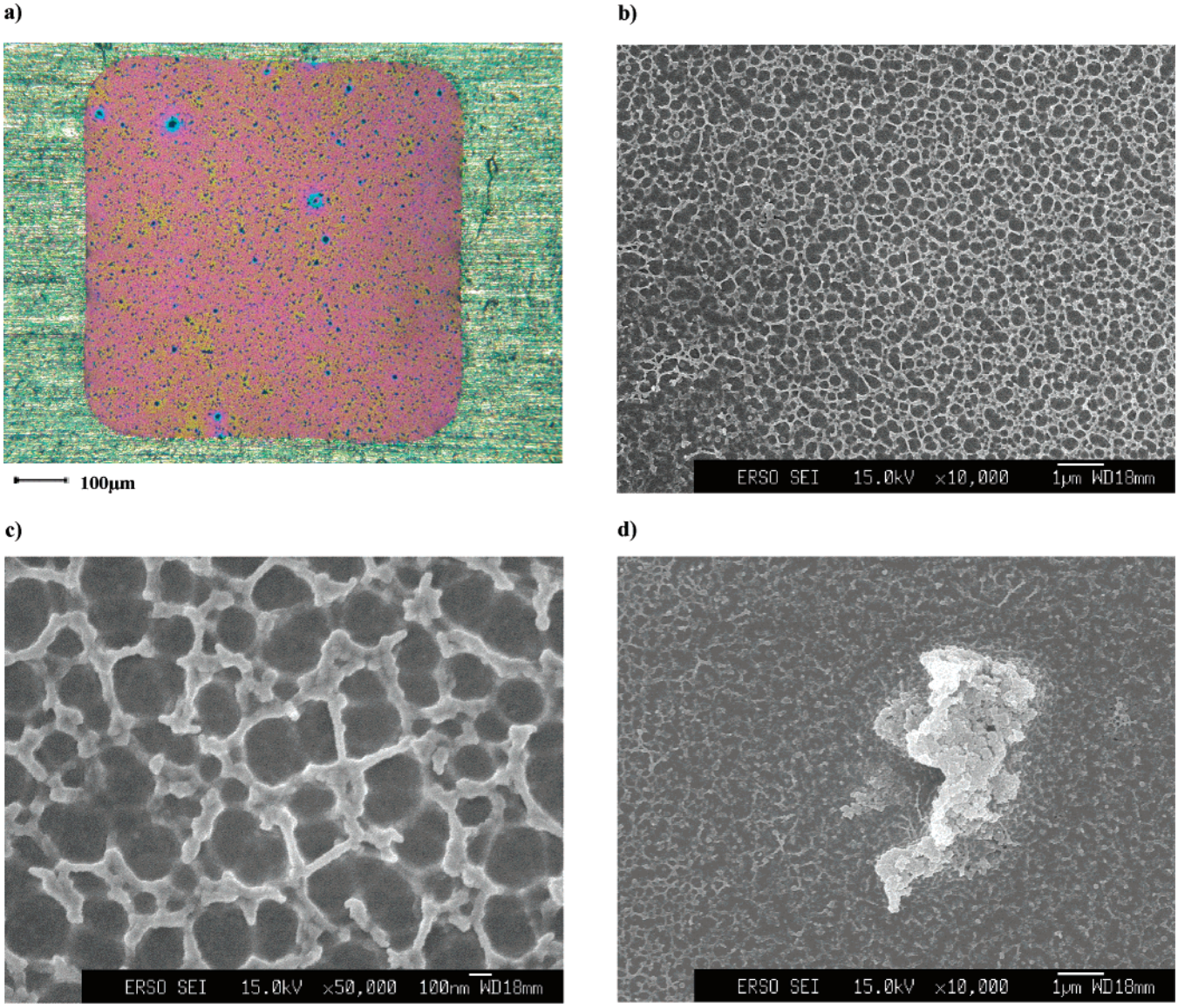

Figure 2. (a) Optical micrograph MWNT/PS films coated on copper grids, without stretching; and (b,c,d) SEM micrograph of the plasma-etched MWNT/PS film showing the nanotube network (in b and c) and aggregates (in d).

Instrumental, Nanoscope IIIa) to investigate the nanotopographic information. The AFM topographic data were used to calculate the local nanomechanical information in the local deformation zones.[24,25] A field emission scanning electron

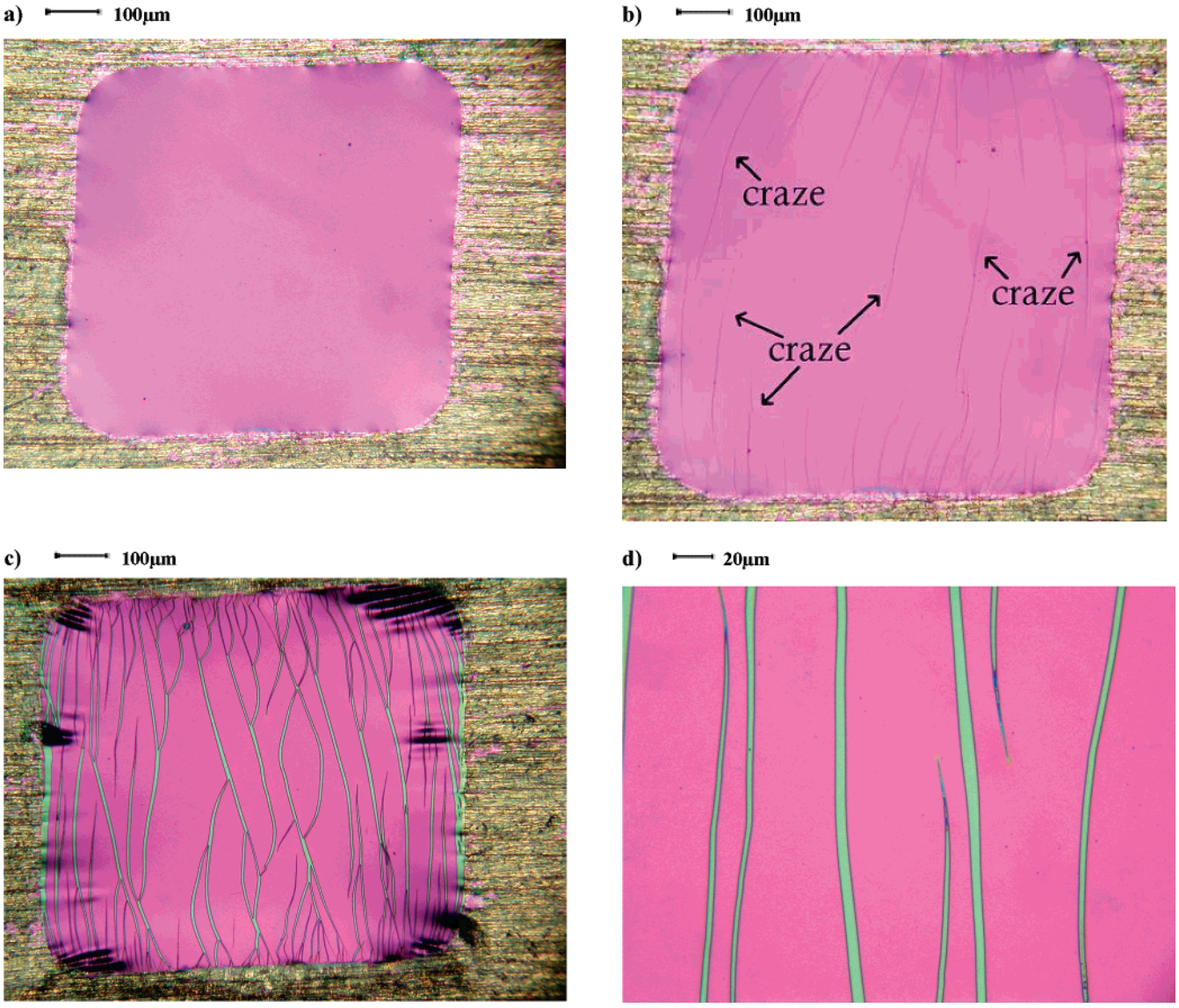

Figure 3. Optical micrograph of pristine PS films coated on copper grids: (a) without stretching, (b) with crazes (some marked with arrows) just initiated, (c) local craze breakdown, and (d) crazes at a higher magnification.

microscopy (FE-SEM) system (JEOL JSM-6500) was then used to observe the surfaces of MWNT/PS films. Scanning transmission electron microscopy (STEM, JEOL 200CX) was used to observe the microstructures of the MWNT/PS films. Pristine polystyrene (PS, M_w = 2 000 000) films (0.5 μm thick) were prepared as a control for the experiment.

Results and Discussions

Nanotube Dispersion in Solid Films. The nanocomposite thin films of MWNT/PS showed excellent mechanical properties, indicative of a generally well-dispersed, percolated network of MWNTs embedded in the polymer matrix. Nevertheless, sporadic MWNTs aggregates were spotted under an optical microscope, and the surface of the MWNT/PS films was significantly rougher than the pristine PS (Figures 2a and 3a). The dispersion of the MWNTs in the polymer thin film was further explored by conducting a separate experiment using oxygen plasma to mildly etch the nanocomposite films. A uniform network of MWNT covered by molten polymer emerged after etching (Figures 2b and 2c), attributable to a large difference in etching rate between polymer and carbon nanotubes. The average external diameter of the emerged nanotubes was consistent with the original specification of around 30 nm. Furthermore, the "mesh size" of the nanotube network was around 200−300 nm. Sporadic aggregates were found on the etched surface (Figure 2d), which appeared to be fused nanotubes. As a comparison, the etched surface of the pristine PS film was clean and smooth.

Effects on Microscopic Deformation Behavior. It is well-known that local deformation zones grow in neat polymer glasses upon stretching by tensile stresses. The deformation zones were categorized into crazes (the brittle mode) or shear deformation zones (the ductile mode).[4] Crazes were characterized with an interconnected fibrillar structure,[4] while shear deformation zones were local regions monotonically thinned. In the control experiment of pristine PS films, crazes were usually initiated near the edges of the film squares or local defects such as dust particles or aggregates (Figure 3b). After the initiation of crazes at approximately 1% strain (the crazing strain ϵ_c), most further deformation was concentrated toward the preexisting crazed areas, and the regions outside the crazes were subjected to virtually no strain beyond ϵ_c.[4] The crazes were generally straight, widening steadily as the strain increased, and

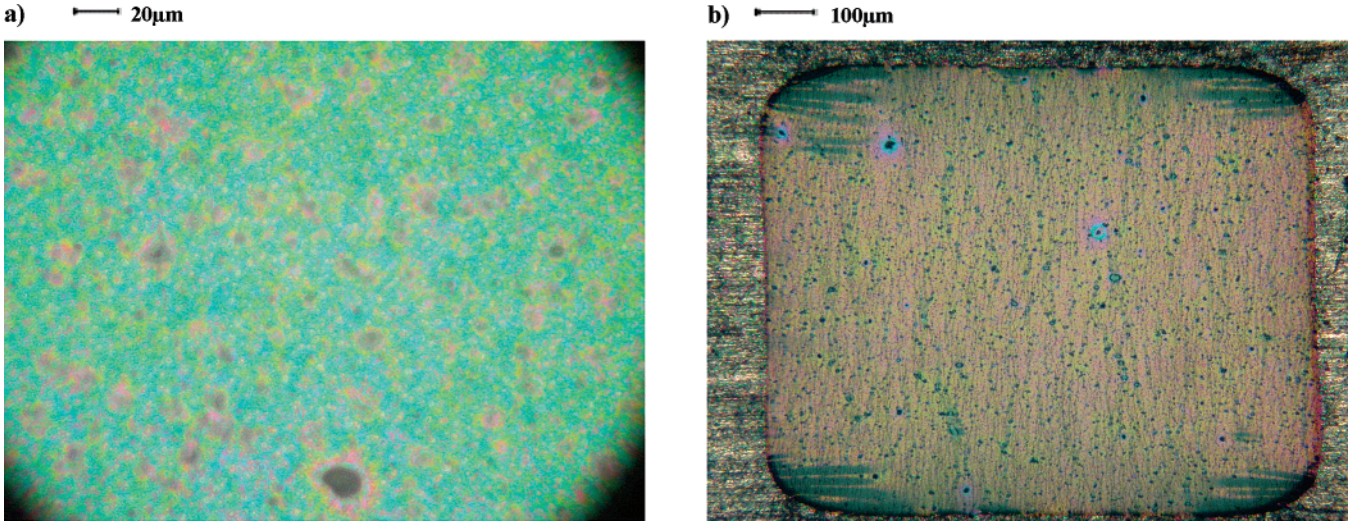

Figure 4. Optical micrograph of MWNT/PS films coated on copper grids: (a) local deformation zones initiated at 1.2% strain (the black spot at the bottom is a nanotube aggregate) and (b) many tiny local deformation zones at 23.5% strain.

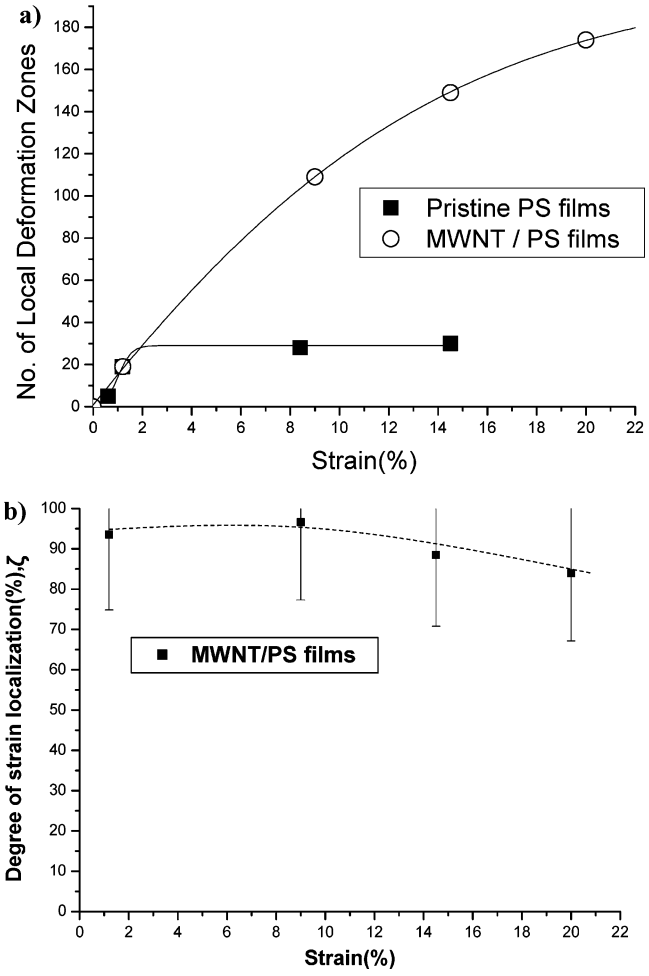

Figure 5. (a) Number of local deformation zones vs strain in the pristine PS and MWNT/PS films, (b) the degree of strain localization ζ vs the strain in the MWNT/PS films.

effectively absorbing the externally applied deformation into the tiny zones (Figures 3c and 3d). Very few new crazes were nucleated after 1.5% strain (Figure 5a). As strain increased further, local fibril breakdowns within the crazes began at approximately 8% strain,[10] and the maximum width of crazes could reach approximately 18 μm as determined from AFM surveys.

In contrast, the MWNT/PS films showed a very different behavior. In the MWNT/PS films, the emergence of tiny local deformation zones occurred at a critical strain at around 1.2% (Figure 4b). As the strain increased, the development of the tiny local deformation zones was effectively suppressed with the zone width increased only slightly (Figures 4c and 4d). At the same time, however, a large number of new local deformation zones were initiated as the strain increased. Up to the point of maximum strain where the supporting copper grids broke at 23.5% strain, virtually all the local deformation zones in the film remained short and narrow (less than 2 microns wide). Very few local breakdowns were observed, and if there were, primarily because of aggregates, the microvoids were readily arrested. These results strongly indicated that the MWNT networks embedded in the PS film effectively retarded the growth and broadening of the local deformation zones and thus increased dramatically the toughness of the glassy polymer.

To further examine the effect of MWNTs network on the nanoscopic mechanical properties, the number of the tiny local deformation zones in the stretched sample was counted as a function of the applied strain (Figure 5a). In the pristine PS film, the number of crazes increased only in the range of low strains; it quickly leveled off as the strain increased, reflecting the fact that crazes act as strain sinks in these films. However, in the MWNT/PS films, the number of local deformation zones increased steadily with strain and started to level off only when the strain exceeded ~15%. The number of local deformation zones in MWNT/PS films was approximately 7 times of that of crazes in pristine PS films at $\epsilon = 20\%$.

To quantify the role of strain sink played by the local deformation zones, an empirical parameter ζ for gauging the degree of strain localization[26] was defined as the ratio of the total cumulative width of local deformation zones projected along the strained direction to the total sample width. If $\zeta = 0$, strain was entirely bore by the matrix outside the deformation zones with no strain localization, while $\zeta = 100\%$, on the other hand, indicated that entire deformation was absorbed in the deformation zones. It was found that, for the MWNT/PS films, ζ reached to a level greater than 90% at 2% strain, indicating that nearly all the applied deformation

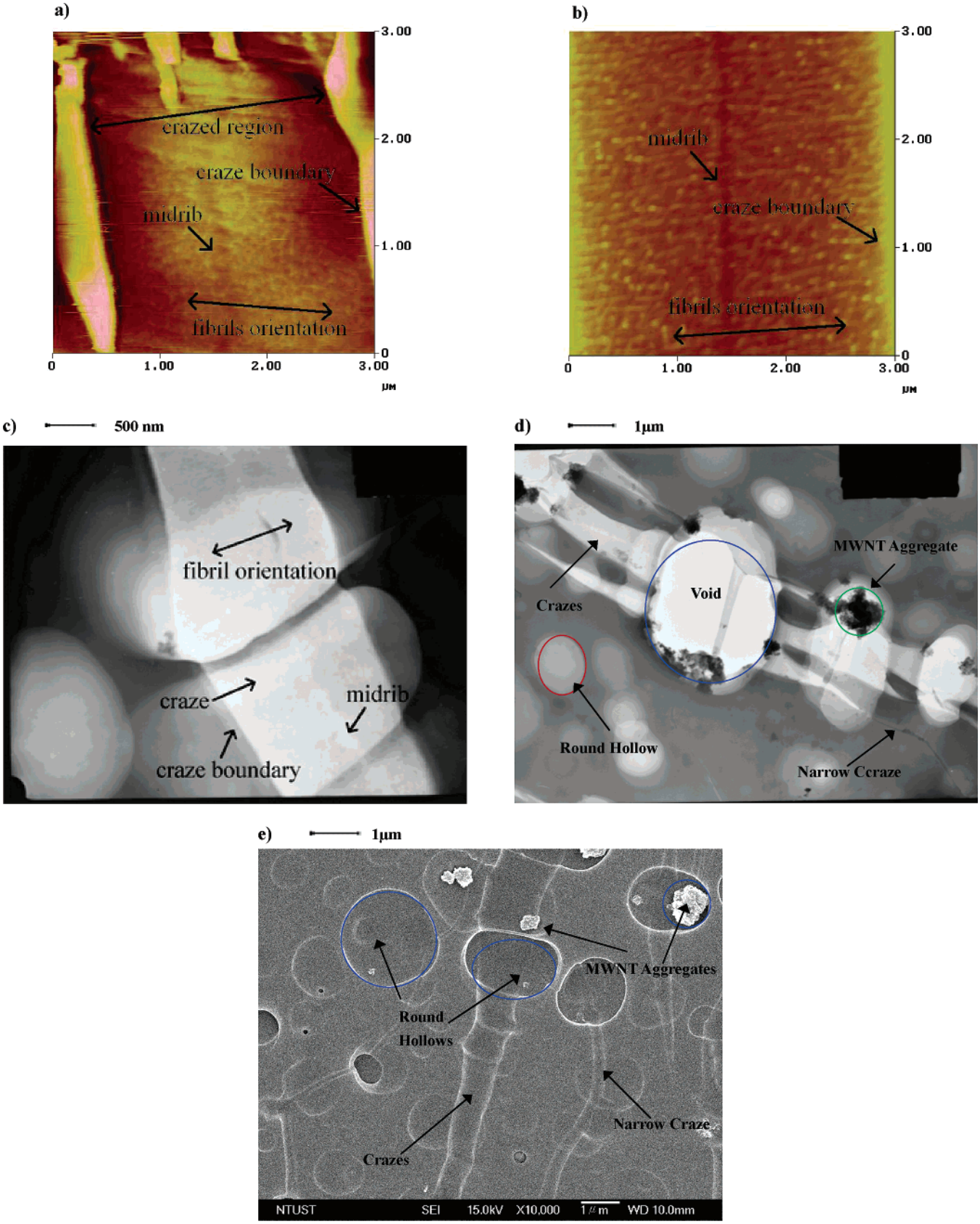

Figure 6. (a) AFM micrograph of crazes in pristine PS films at 14.5% strain; and (b) AFM micrograph of crazes in MWNT/PS films at 23.5% strain, (c) TEM micrograph of a craze in MWNT/PS films, (d) TEM micrograph of stretched MWNT/PS films (23.5% strain), and (e) SEM micrograph of stretched MWNT/PS films at 23.5%.

concentrated in the local deformation zone as soon as the deformation zones were initiated (Figure 5b). As the strain increased to greater than 10% strain, ζ decreased somehow to approximately 85%. Although coming with a large experimental error bar, it seemed to suggest that the region outside the deformation zones started to participate in strain sharing for about 10−15% of the total deformation.

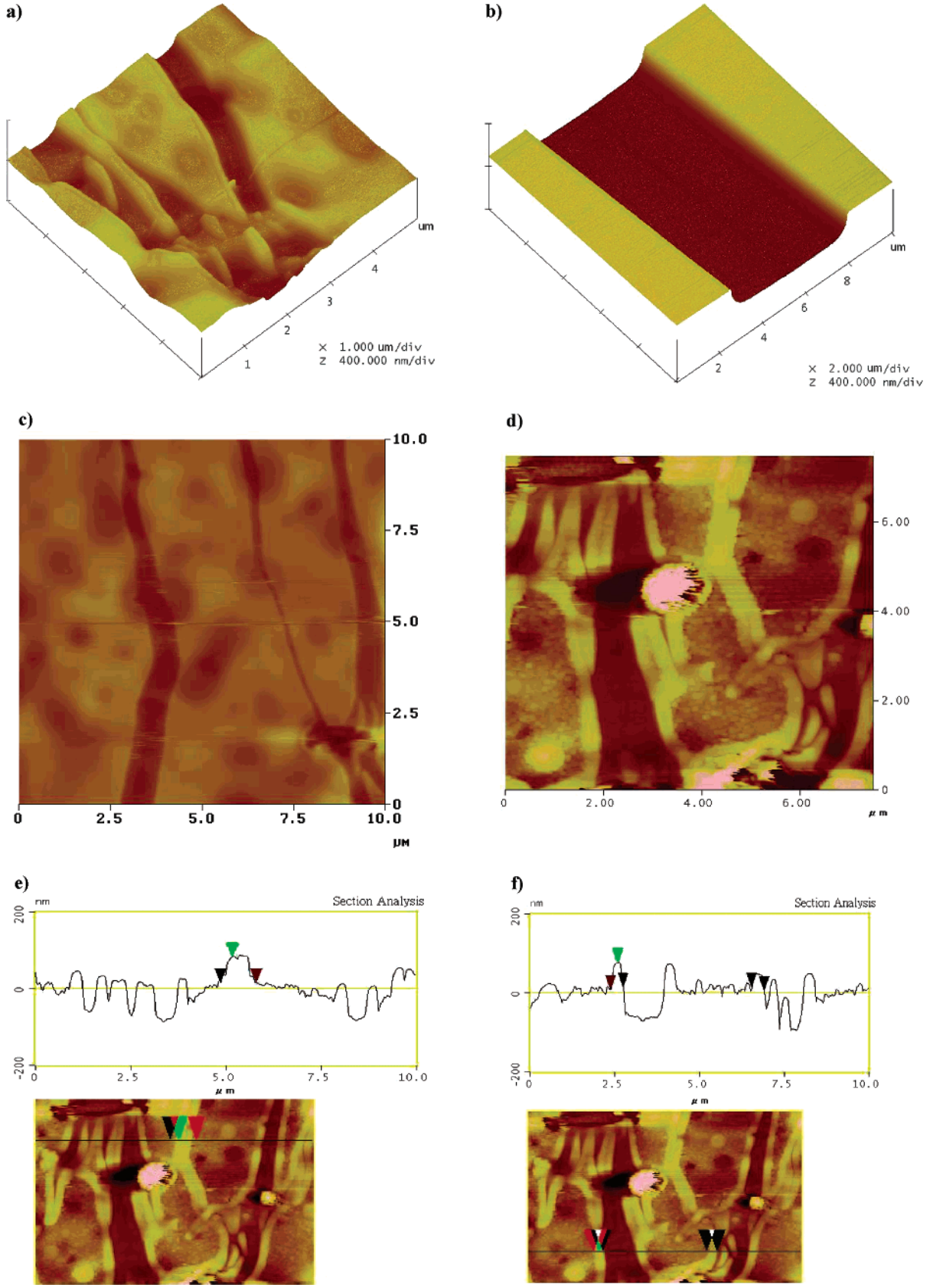

Figure 7. (a) Craze surface topography in MWNT/PS films, (b) craze surface topography in pristine PS films, (c) AFM micrograph of stretched MWNT/PS films without plasma etching, (d) AFM micrograph of stretched and etched MWNT/PS film, and (e, f) sectional topographical analyses at different locations of the MWNT/PS films.

Microstructure and Micromechanics of the Local Deformation Zones. The microstructure of the local deformation zones were examined under AFM (Figure 6a) and TEM (Figure 6c), and a fibrillar structure was observed, indicating that the tiny local deformation zones are crazes (Figure 6b). A midrib[4] was observed in the central line of the local deformation zones, which was the locus traced behind the craze tip

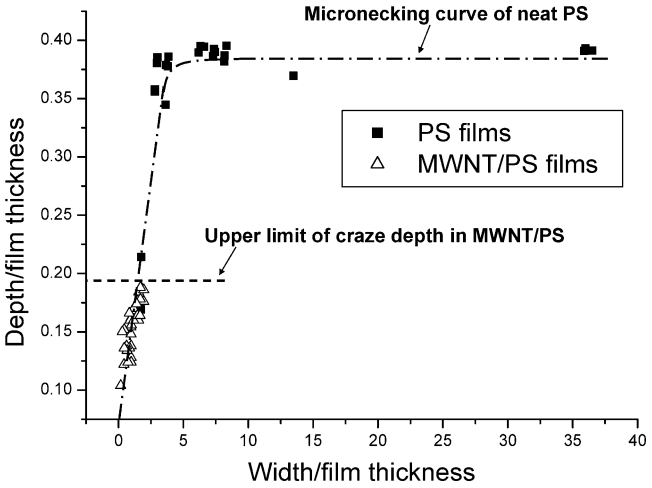

Figure 8. Craze depth d vs craze width w in the pristine PS and MWNT/PS films.

during craze propagation. The highly strained fine features was found to have a width of approximately 70−100 nm in the nanocomposite crazes. The microstructure and the midrib width observed in MWNT/PS films were similar to that found in pristine PS crazes.

Attempts were made to investigate the state of the drawn MWNTs within crazes. However, probably because of poor contrast, no individual MWNTs were observed in the crazed regions (Figure 6c). Rather, aggregates apparently composed of MWNTs were observed, which probably acted as the craze initiators (Figure 6d). Investigation with SEM on the surfaces of the nanocomposite films also yielded no observations of the individual nanotubes (Figure 6e). On the surfaces of the films, however, small, round depressions were found by SEM (Figure 6e). This was consistent with the observed light spherical spots in the TEM micrographs (Figure 6d). These features were thought to be either regions of low mass density or bubbles, the origins of the latter were still unclear.[27−28] The topography of the crazed MWNTs/PS films (Figure 7a) was compared further with that of the neat PS (Figure 7b) by using AFM. The surface of the pristine PS film was quite flat and smooth except for the crazed regions where depressions due to local thinning were found. In contrast, the MWNT/PS film surface was generally rough, and the crazes, usually quite narrow and winding, traveled up and down laboriously on the uneven surface (Figure 7a and c). Craze growth in the neat polymer was shown previously to follow a micronecking process, in which the craze depth d increased linearly with craze width w until the width reached a critical value w_c beyond which the depth remained constant.[2−3] The critical craze width w_c is around 2.5 μm for 0.5 μm thick PS films. Figure 7b shows a section of the mature craze in pristine PS film with a width around 5 μm and a depth approximately one-third of the film thickness. The craze depth of MWNTs/PS crazes was found to follow the same d versus w curve when normalized to the film thickness, apparently following the same micronecking process (Figure 8). The width of the crazes in MWNTs/PS films, however, never reached w_c, and the craze depth was capped at about 19% of the film thickness. This hardened behavior apparently was due to the influences of the embedded MWNTs in the polymer film.

In an attempt to reveal the effect of MWNTs on the development of crazes, some of the crazed samples were mildly etched by oxygen plasma to expose the underlying arrangement of the MWNTs in the stretched films. The AFM topography and the SEM micrograph of the etched crazed MWNT/PS films were illustrated in Figures 7d and 9a in comparison to that of the etched crazed pristine PS shown in Figure 9b. In the MWNTs/PS films, protrusions were seen bulging along the banks on both sides of the crazes after plasma etching. These protrusions, however, were not observed in the etched crazed films of neat PS. The height and width of the protruding ridges were 40−70 nm and 350−1000 nm, respectively, as measured by AFM sectional analysis (Figure 7d−f). The ratio of the height to the width of the protrusions was approximately 1:10, indicating that they were mild surface bulges with surface angle ~10° ($\tan^{-1}(1/5)$). Furthermore, extensive examination on the AFM micrographs led to the conclusion that no nanotubes were discovered inside the crazes in the etched sample. This is consistent with the SEM observation of etched crazed samples, where nanotubes were only found outside the crazes[22] (Figure 9a). It was plausible

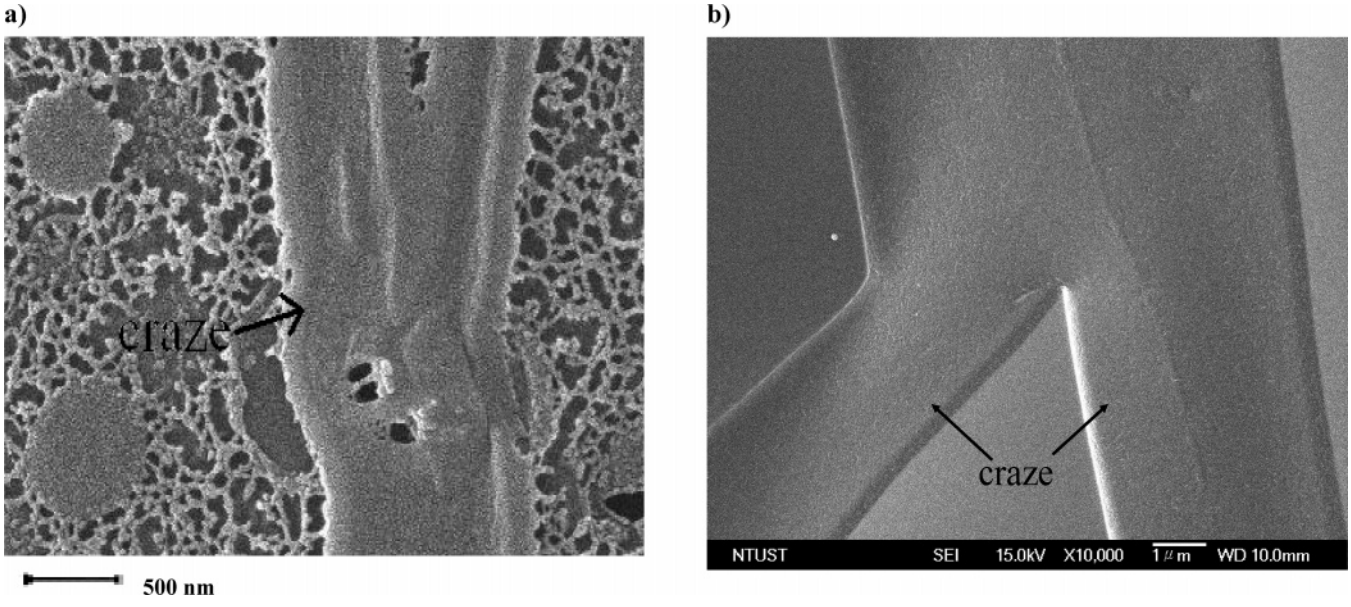

Figure 9. SEM micrographs of etched crazes in: (a) MWNT/PS films, and (b) pristine PS films.

to infer that crazes were predominately initiated in the regions where nanotube density was low. The protrusions along the craze boundaries could be a result of mechanical interactions between the nanotubes network and the polymer chains during craze growth. More detailed analyses and research work would be required to further unveil the molecular process of crazing in the MWNT/PS films. The local true stress and strain associated with the fibrillating polymer chains at the nanoscales can be determined from the nanotopography of crazes mapped by using AFM.[3]

On the basis of above analyses on the experimental observations, it could be concluded that crazes were largely confined in the regions where the nanotube network were loose or sparse. Once the crazes entered the regions of a well-structured nanotube network, the nanotube restricted the propagation and the widening of the crazes. Since these regions of loose MWNTs in effect were regions of defects, the nanomechanical behavior may become quite different when the dispersion of MWNTs is further improved to eliminate these defects entirely. It is also interesting to investigate the existence of the threshold mesh size of the nanotubes network below which craze nucleation and growth would be completely depressed. We are currently conducting experiments to target these points.

Conclusions

The micromechanical properties of glassy polymer could be enhanced dramatically by adding surface-grafted MWNTs into the polymer matrix. Although crazing (strain localization by fibrillation) remained the dominant microdeformation mechanism and craze widening still followed the same micronecking process, the well-dispersed percolated network of MWNTs significantly restricted the fibrillation process, preventing the maturation of craze fibrillation and hence the breakdown of the fibrils. As a result, nucleation of new crazes became the dominant process over widening of the existing crazes when the applied strain increased. At very large strains, however, the load-bearing percolated network of MWNTs outside the crazes seemed to start to participate in sharing the applied strain. Preliminary data indicated that very few MWNTs were drawn into crazes and most of them were piling up at the craze boundaries, a result consistent with the large difference in rigidity between the MWNTs and polymer chains.

Acknowledgment. We deeply appreciate the financial support of the National Science Council of Taiwan and a grant from the US Air Force (AOARD-04-4074).

Note Added after ASAP Publication. This article was released ASAP on April 21, 2005 with an author name spelled incorrectly. Chen-Chi M. Mar has been revised to Chen-Chi M. Ma. The correct version was posted on April 21, 2005.

References and Notes

(1) Ward, I. M. *Mechanical Properties of Solid Polymers*, 2nd ed.; John Wiley & Sons Press: New York, 1983.
(2) Lin, J.-H.; Yang, A. C.-M. *Macromolecules* **2001**, *34*, 4865.
(3) Lin, J.-H.; Yang, A. C.-M. *Macromolecules* **2001**, *34*, 3698.
(4) Kramer, E. J. *Adv. Polym. Sci.* **1983**, *52/53*, 1.
(5) Yang, A. C.-M.; Wang, R. C.; Kunz, M. S.; Yang, I, C. *J. Polym. Sci., Polym. Phys. Ed*. **1996**, *34*, 1141.
(6) Kaush, H. H. *Polymer Fracture*; Springer-Verlag: Heidelberg, Germany, 1978.
(7) Donald, A. M.; Kramer, E. J. *Polymer* **1982**, *23*, 457.
(8) Donald, A. M.; Chan, T.; Kramer, E. J. *J. Mater. Sci*. **1981**, *16*, 669.
(9) Yang, A. C.-M.; Kramer, E. J. *J. Polym. Sci., Polym. Phys. Ed.* **1985**, *23*, 1353.
(10) Yang, A. C.-M.; Kramer, E. J.; Kuo, C. C.; Phoenix, S. L. *Macromolecules* **1986**, *19*, 2010.
(11) Yang, A. C.-M.; Kramer, E. J.; Kuo, C. C.; Phoenix, S. L. *Macromolecules* **1986**, *19*, 2020.
(12) Yang, A. C.-M.; Kunz, M. S.; Logan, J. A. *Macromolecules* **1993**, *26*, 1767.
(13) (a) Treacy, M. M. J.; Ebbesen, T. W.; Gibson, J. M. *Nature* **1996**, *381*, 678. (b) Yakobson, B. I.; Brabec, C. J.; Bernholc, J. *Phys. Rev. Lett.* **1996**, *76*, 2511.
(14) Dalton, A. B.; Collins, S.; Muñoz, E.; Razal, J. M.; Ebron, V. H.; Ferraris, J. P.; Coleman, J. N.; Kim, B. G.; Baughman, R. H. *Nature* **2003**, *423*, 703.
(15) Cadek, M.; Coleman, J. N.; Barron, V.; Hedicke, K.; Blau, W. J. *Appl. Phys. Lett.* **2002**, *81*, 5123.
(16) Kilbride, B. E.; Coleman, J. N.; Fournet, P.; Cadek, M.; Drury, A.; Blau, W. J. *J. Appl. Phys*. **2002**, *92*, 4024.
(17) Sandler, J. K. W.; Kirk, J. E.; Kinloch, I. A.; Shaffer, M. S. P.; Windle, A. H. *Polymer* **2003**, *44*, 5893.
(18) Biercuk, M. J.; Llaguno, M. C.; Radosavljevic, M.; Hyun, J. K.; Fischer, J. E.; Johnson, A. T. *Appl. Phys. Lett*. **2002**, *80*, 2767.
(19) Wei, C.; Srivastava, K.; Cho, K. *Nano Lett*. **2002**, *2*, 647.
(20) Qian, D.; Dickey, E. C. *Appl. Phys. Lett.* **2000**, *76*, 2868.
(21) Cadek, M.; Coleman, J. N.; Ryan, K. P.; Nicolosi, V.; Bister, G.; Fonseca, A.; Nagy, J. B.; Szostak, K.; Béguin, F.; Blau, B. J. *Nano Lett.* **2004**, *4*, 353.
(22) Lin, T. S.; Hsiao, C. C.; Cheng, L. Y.; Yang, A. C.-M. Submitted.
(23) Lauterwasser, B. D.; Kramer, B. J., *Philos. Mag.* **1797**, *A39*, 469.
(24) Bridgman, D. W. *Studies in Large Plastic Flow and Fracture*; Harvard University Press: Cambridge, 1964; p 9.
(25) G'sell, C.; Marquez-Lucero, A. *Polymer* **1993**, *34*, 2740.
(26) Lin, C. H.; Yang, A. C.-M. *J. Mater. Sci*. **2000**, *35*, 4231.
(27) Watts, P. C. P.; Hsu, W. K.; Chen, G. Z.; Fray, D. J.; Kroto, H. W.; Walton, C. R. M. *J. Mater. Chem.* **2001**, *11*, 2482.
(28) Hsu, W. K.; Kotzeva, V.; Watts, P. C. P.; Chen, G. Z. *Carbon* **2004**, *42*, 1707.

MA048413Y